# Spin-Selective Electron Quantum Transport in Nonmagnetic MgZnO/ZnO Heterostructures

D. Maryenko,[1,*] J. Falson,[2] M. S. Bahramy,[1,2] I. A. Dmitriev,[3,4] Y. Kozuka,[2] A. Tsukazaki,[5] and M. Kawasaki[1,2]
[1]RIKEN Center for Emergent Matter Science (CEMS), Wako 351-0198, Japan
[2]Department of Applied Physics and Quantum-Phase Electronics Center (QPEC), The University of Tokyo, Tokyo 113-8656, Japan
[3]Max Planck Institute for Solid State Research, D-70569 Stuttgart, Germany
[4]A. F. Ioffe Physico-Technical Institute, 194021 St. Petersburg, Russia
[5]Institute for Materials Research, Tohoku University, Sendai 980-8577, Japan
(Received 26 March 2015; published 5 November 2015)

We report magnetotransport measurements on a high-mobility two-dimensional electron system at the nonmagnetic MgZnO/ZnO heterointerface showing distinct behavior for electrons with spin-up and spin-down orientations. The low-field Shubnikov–de Haas oscillations manifest alternating resistance peak heights which can be attributed to distinct scattering rates for different spin orientations. The tilt-field measurements at a half-integer filling factor reveal that the majority spins show usual diffusive behavior, i.e., peaks with the magnitude proportional to the index of the Landau level at the Fermi energy. By contrast, the minority spins develop "plateaus" with the magnitude of dissipative resistivity that is fairly independent of the Landau level index and is of the order of the zero-field resistivity.

DOI: 10.1103/PhysRevLett.115.197601 PACS numbers: 77.55.hf, 71.70.-d, 72.25.Rb, 73.43.Qt

The understanding of electron scattering mechanisms is a fundamental problem in the quantum transport of two-dimensional (2D) charge carrier systems. Moreover, the knowledge about the scattering mechanisms may serve as a guiding line for improving the design of the heterostructures and adjusting their growth conditions [1–3]. Shubnikov–de Haas oscillations (SdHOs) are one instance of charge carrier scattering in the magnetic field and, on a simplified level of consideration, carry the information about the small angle scattering and charge carrier mass. The SdHO shape in a 2D system is frequently approximated within the Lifshitz-Kosevitch (LK) model adopted from the original description of three-dimensional transport [4]. This description is valid for a uniform system and in the absence of interactions. While the electron-electron interaction and the sample's inhomogeneity in the regime of small amplitude oscillations have been gradually accounted for [5–11], in a stronger magnetic field the electron transport becomes sensitive both to correlation properties of disorder and to ferromagnetic exchange interaction, which are difficult to take into account simultaneously [9,12,13]. The quantum transport analysis becomes nontrivial and the unraveling of individual contributions is very challenging. Yet, on a phenomenological level, valuable information can be gained about the properties of the underlying 2D system.

In this Letter, we report experimental studies of SdHO in the MgZnO/ZnO heterostructure confined two-dimensional electron system (2DES) [3,14,15]. We find an electron spin-dependent scattering with the spin-down (↓) electrons (having higher Zeeman energy and thus forming the spin minority) being more prone to scattering than the spin-up (↑) electrons (having lower Zeeman energy). Figure 1 exemplifies the most remarkable phenomena in our study. The longitudinal resistance $R_{xx}$ at half-integer Landau level (LL) filling factor $\nu = (nh/eB_{\perp})$, where $n$ is the charge carrier density, changes stepwise as the in-plane field component $B_{\parallel}$ increases, and the high (low) $R_{xx}$ correlates with ↑ (↓) spin-orientation electrons at the chemical potential $\mu$. While $R_{xx}$ for ↑ orientation gradually increases with $B_{\parallel}$, $R_{xx}$ for ↓ orientation develops a series of flat regions (plateaus) with $R_{xx}$ magnitude that is fairly independent of the LL index and is on the order of $R_{xx}$ at $B = 0$. As we show below, the minority spins do not obey the diffusive model. A similar behavior is indicated in AlAs heterostructures [16]. However, owing to the measurements at low $\nu$, only one $R_{xx}$ minimum for each $\nu$ has been measured with the sizable different magnitudes.

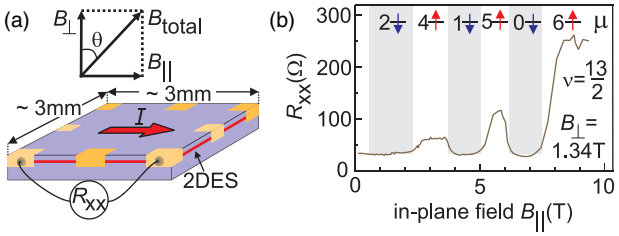


FIG. 1 (color online). (a) Schematic view of the sample geometry and the magnetic field orientation. (b) Example of $R_{xx}$ dependence on $B_{\parallel}$ at half-integer $\nu$. The LL index $N$ and the spin state at the chemical potential $\mu$ are indicated. $R_{xx}$ for electrons with ↓-spin orientation at $\mu$ is independent of $B_{\parallel}$, while $R_{xx}$ for ↑ spin increases gradually. Such behavior is also found at other half-integer $\nu$.

 

We start with the description of SdHO for $B_{\parallel} = 0$. Figure 2 represents characteristic SdHO examples for several structures. The oscillation minima correspond to odd $\nu$ before the splitting due to the electron level arrangement in $B_{\perp}$ as shown in the inset in Figs. 2(a)–2(c) [17–19]. The SdHO splitting corresponds to the resolving $\uparrow$ and $\downarrow$ electron spin states and develops rapidly on the $B_{\perp}$ axis. This suggests that the exchange interaction strongly affects the splitting [9,11,20]. After splitting, the SdHO displays a distinct pattern of alternating heights of $R_{xx}$ maxima. This is an inherent feature of high-quality MgZnO/ZnO heterostructures. Alternating $R_{xx}$ peak heights have also been seen in other 2DESs [5,9,21–23]. Two envisioned SdHO envelopes (red and blue dashed lines) can be intuitively interpreted as distinct scattering for two spin states. The LK formalism captures well this behavior on a phenomenological level when two scattering times are assumed each for one-spin orientation ($\tau_{\uparrow}$ and $\tau_{\downarrow}$). We do not consider the interaction effects, which can damp SdHO [5,7,11,24]. Then the correction to the magnetoresistance due to SdHO reads within the LK model

$$\frac{\Delta R_{xx}}{R_{xx}} = 2\sum_{r,\uparrow,\downarrow} \frac{rX}{\sinh(rX)} \exp\left(-r\frac{\pi}{\omega_c \tau_{\uparrow,\downarrow}}\right) \cos\left(r\phi_{\uparrow,\downarrow}\right), \tag{1}$$

where $\omega_c = eB_{\perp}/m^*$ is the electron cyclotron frequency with spin-independent mass $m^* = 0.3m_0$ and $X = 2\pi^2 k_B T/\hbar\omega_c$ depends on the temperature $T$. The phase $\phi_{\downarrow,\uparrow} = 2\pi(E_F/\hbar\omega_c)\{1 \pm [(g^*\mu_B B_{\text{total}})/(2E_F)]\} - \pi$ includes the Zeeman component with $g^*$ being the electron Landé $g$ factor and the Fermi energy $E_F$ at $B_{\text{total}} = 0$.

The brown lines in Figs. 2(a)–2(c) obtained with Eq. (1) considering $r = 1 \ldots 15$ reproduce well the SdHO shapes with parameters given in the figure's caption. A deviation occurs at higher fields which may be associated with the non-Lorentzian shape of LLs and the Zeeman splitting being comparable to $E_F$. Most importantly, however, the simplified LK model captures the alternating $R_{xx}$ heights due to different $\tau_{\uparrow}$ and $\tau_{\downarrow}$. A larger $R_{xx}$ (envelope of larger oscillation amplitude) is given by a larger $\tau$ for the $\uparrow$ state, while a smaller $R_{xx}$ (envelope of smaller oscillation amplitude) is reproduced with a smaller $\tau$ for the $\downarrow$ state. The difference between $\tau_{\uparrow}$ and $\tau_{\downarrow}$ is observed at all temperatures and in all samples; see Fig. 2(d). This establishes the presence of a scattering mechanism acting selectively on the electron spin orientation. Since we consider the regime of the classical Hall effect, in which the bulk properties of 2D are probed, the edge-state transport model is not the prime mechanism for spin-dependent transport [25,26]. The temperature increase of $1/\tau$ in Fig. 2(e) for the samples with the two lowest $n$ is consistent with the correction $\delta\tau^{-1} \equiv \tau_{\uparrow,\downarrow}^{-1} - \tau_{T=0}^{-1} \propto T/E_F$ due to the interplay of the electron-electron interaction and disorder scattering [7]. This effect is less pronounced in the highest electron density sample, where the interaction effects are expected to be weakest and the disorder to be different [3]. The best description of SdHO is achieved with the spin susceptibility ($g^*m^*$), which is lower than measured in our previous experiments [17–19]. This likely originates from the fact that our simplified SdHO model does not properly account for interaction effects [9,11,20]; see Supplemental Material [27].

To further investigate the origin for the spin-selective scattering, the sample in Fig. 2(b) is rotated in the magnetic field. This allows the independent control of the orbital and spin degrees of freedom. Figure 3(a) displays the $R_{xx}$ color rendition as a function of $\nu$ and $1/\cos(\theta)$. As reported previously [19], in the color rendition of $R_{xx}$, changes are associated with the multiple LL crossings, which are traced from the level diagram sketched in Fig. 3(d). The LL index $N$ and spin orientation, at which the chemical potential $\mu$ resides, are overlaid for a number of regions. The areas with

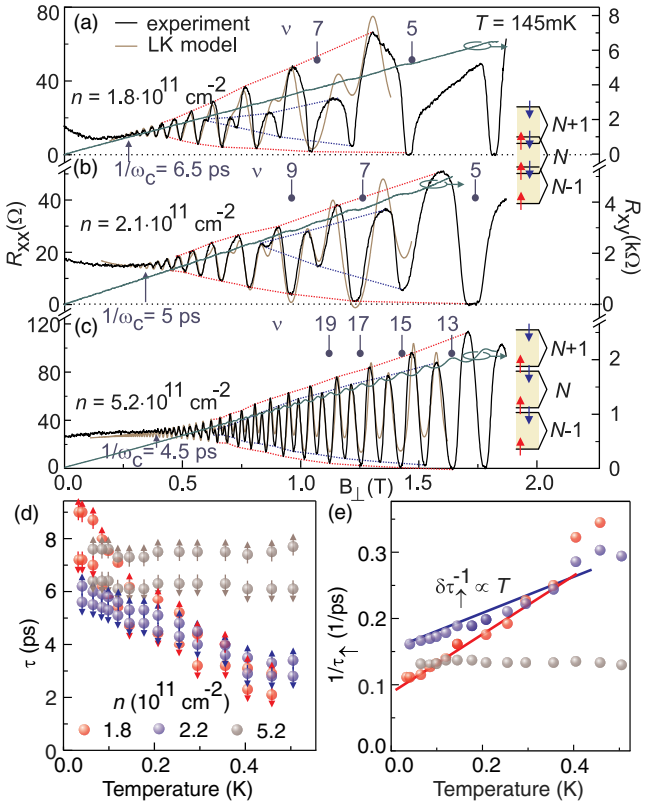


FIG. 2 (color online). SdHO in MgZnO/ZnO heterostructures at $B_{\parallel} = 0$. A reversed sequence of $R_{xx}$ maxima in (c) in comparison to (b) signals that the first coincidence did not occur in $B_{\parallel} = 0$. Brown lines evaluated with Eq. (1) reproduce the alternating peak heights using the following parameters: an electron mass $m^* = 0.3m_0$ and a $g$ factor (a) $g^* = 4.2$, (b) $g^* = 3.9$, and (c) $g^* = 3.7$. The scattering times are (a) $\tau_{\uparrow} = 6.2$ ps, $\tau_{\downarrow} = 4.7$ ps, (b) $\tau_{\uparrow} = 5.3$ ps, $\tau_{\downarrow} = 4.8$ ps, and (c) $\tau_{\uparrow} = 7.4$ ps, $\tau_{\downarrow} = 6.1$ ps. (d) Temperature dependence of $\tau_{\uparrow}$ and $\tau_{\downarrow}$ extracted from SdHO analysis. (e) The linear correction $\delta\tau^{-1} \propto T$ implies a contribution of electron-electron interaction.

the assigned ↓ state have a lower resistance (blue) than the regions with ↑ state (red). This behavior is traced down to $\theta = 0$ and implies a common origin for the spin-dependent scattering.

We apply the LK model to analyze the $R_{xx}$ traces at several tilt angles and explore the $\tau$ change with $\theta$. Figure 3(c) depicts $R_{xx}$ traces versus $\nu$ for three representative $\theta$'s. Unlike the case $\theta = 0$, the SdHOs cannot be described with a field-independent $\tau_\uparrow$ and $\tau_\downarrow$. For reproducing the SdHO, a phenomenological dependence $\tau_\uparrow = \tau_0(1 + \gamma_1 B_{\text{total}})$ and $\tau_\downarrow = \tau_0(1 + \gamma_2 B_{\text{total}})$ is assumed with $\gamma_1 = 0.15$ and $\gamma_2 = 0.05$ describing the $\tau$ increase rate with $B_{\text{total}}$ [5]. The enhancement of $\tau_\uparrow$ with $B_{\text{total}}$ seizes the increase of oscillation amplitude at smaller $\nu$. The LK model fails to capture the behavior for the ↓ state, and, overall, the description of SdHO becomes worse for larger $\theta$. A severe difference between $\tau_\uparrow$ and $\tau_\downarrow$ in the tilted field emphasizes the selectivity in spin transport. At $\theta$'s, when 2DES has several spin-polarized LLs, the LK model can again describe the $R_{xx}$ oscillations. Figure 3(b) exemplifies the trace at $\theta = 85.8°$, which represents SdHO of a spin-polarized system between $\nu = 14$ and $\nu = 8$. This region is described with a field-independent $\tau = 5.3$ ps.

We now scrutinize the region at low $\nu$, where the agreement between the experiment and the LK model becomes worse. Figure 4(a) examines how $R_{xx}$ changes with $1/\cos(\theta)$ at $\nu = 5 + 1/2$ and $\nu = 6 + 1/2$ and shows the arrangement of occupied LLs. The high (low) $R_{xx}$ correlates with the electron ↑ (↓) states at $\mu$; while $R_{xx}$ for the ↑ state increases with $1/\cos(\theta)$, $R_{xx}$ for the ↓ state remains largely independent of $1/\cos(\theta)$. Such a behavior holds true for other half-integer $\nu$'s; see Fig. 4(b). The increase of $R_{xx}$ with $1/\cos(\theta)$ is consistent with the model of diffusive transport between integer $\nu$'s [28,29]. In this model, the peak resistivity is $R_{\max}^{(\text{th})} \simeq h/(e^2\nu^2) \times (N_\uparrow + 1/2)\tau_\uparrow/\tau_{\text{tr}}$, where $\tau_{\text{tr}}$ is the transport scattering time. Here, we (i) assumed two spin channel parallel conduction, $\sigma_{xx} = \sigma_{xx,\uparrow} + \sigma_{xx,\downarrow}$, (ii) took into account $\sigma_{xx,\uparrow} \gg \sigma_{xx,\downarrow}$ at maxima, since $\mu$ resides in the center of the $N_\uparrow$ LL, and (iii) used the relation $R_{xx} \simeq \sigma_{xx}(h/\nu e^2)^2$ due to $\sigma_{xy} = \nu e^2/h \gg \sigma_{xx}$. Figure 4(c) illustrates the relation between $R_{xx}$ local maxima, $R_{\max}^{(\text{exp})}$, extracted from traces in Fig. 4(b), and the theoretically expected $R_{\max}^{(\text{th})}$ considering $\tau_\uparrow/\tau_{\text{tr}} \sim 0.05$ taken from the sample mobility and the LK analysis. A good agreement between the experiment and the diffusive model is evident. Apparently, the same model does not describe the behavior for ↓ states, since $R_{xx}$ here is independent of $N_\downarrow$ [30]. The dashed lines in Fig. 4(a) illustrate this point by indicating the expectation $R_{\max}^{(\text{exp})}$ values for the ↓ state extrapolated from the above experimental model for ↑ states. Such a contrasting behavior for two spin orientations is further emphasized when one compares the regions (II) and (III) for $\nu = 5 + 1/2$ or (III) and (IV) for $\nu = 6 + 1/2$. It reveals that $R_{xx}$ changes by a factor of 3 solely due to the interchange of

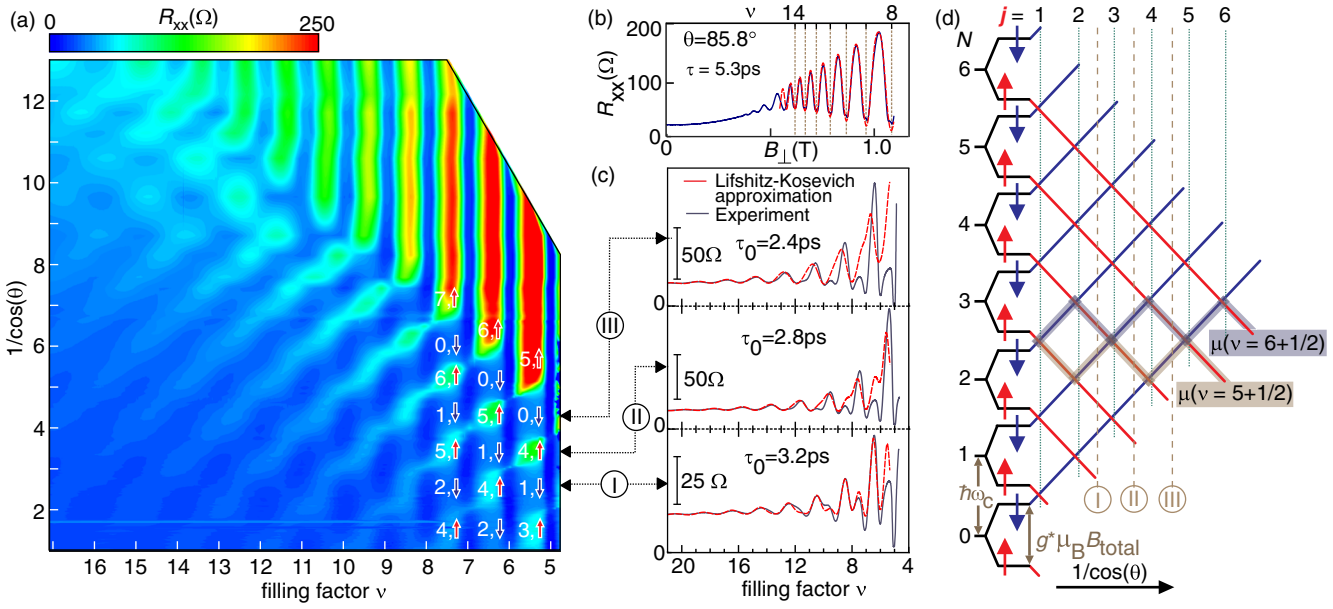


FIG. 3 (color online). (a) Color rendition plot of $R_{xx}$ for the sample in Fig. 2(b) as a function of $\nu$ and $1/\cos(\theta)$ is adopted from Ref. [19]. The LL index $N$ and the electron spin state at the chemical potential $\mu$ are indicated. The analysis of LL crossing yields the spin susceptibility $g^*m^* = 2.0$ [19]. (b) Spin-polarized LLs are formed between $\nu = 14$ and 8 at a large $\theta$. The LK model describes the SdHO considering a field-independent $\tau$. (c) The LK model is applied to describe the SdHO at several $\theta$'s. Here, $\tau_\uparrow$ and $\tau_\downarrow$ are field dependent; see the main text. At large $\theta$, the LK model fails to reproduce the experimental traces. (d) Crossings of spin-resolved LL in a tilted magnetic field given by $1/\cos(\theta)$ at fixed $B_\perp$.

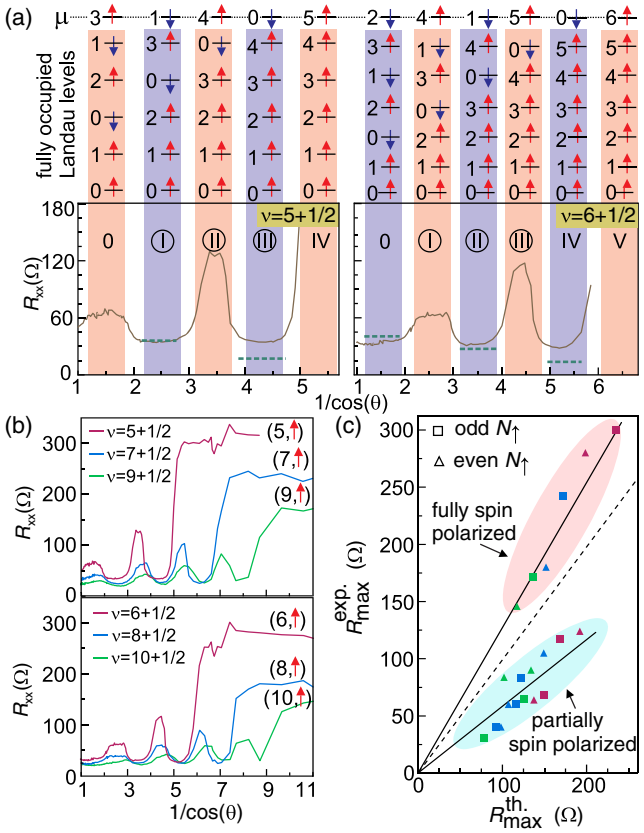


FIG. 4 (color online). (a) $R_{xx}$ versus $1/\cos(\theta)$ for $\nu = 5 + 1/2$ and $6 + 1/2$. The spin configuration is given on top. While $R_{xx}$ for the ↑ state increases with $1/\cos(\theta)$, $R_{xx}$ of the ↓ state remains almost unchanged. An interchange of upper two levels, e.g., regions (II) and (III) for $\nu = 5 + 1/2$, causes a severe resistance change. Dashed lines indicate the expectation $R^{th}_{max}$ values for the ↓-spin diffusive transport. (b) The behavior in (a) is found at other half-integer $\nu$. (c) Linear dependence between local maxima $R^{exp}_{max}$ extracted from (b) and the theoretical expected $R^{th}_{max} = [(\tau_↑/\tau_{tr})(h/e^2\nu^2)](N_↑ + 1/2)$ indicates a diffusive transport for the ↑ spin. Here $\tau_↑/\tau_{tr} = 1/20$. The dashed line represents $R^{exp}_{max} = R^{th}_{max}$. The color of □ and Δ corresponds to color coding in (b).

upper two levels while the other levels remain unchanged. An inspection of regions (0) and (I) for $\nu = 5 + 1/2$ or (I) and (II) for $\nu = 6 + 1/2$ too conforms with the noticeable correlation. Such a dramatic resistance change may point to many-body interaction effects, which take place within the entire 2DES rather than in the vicinity of $\mu$ [5]. It also reminds us of the giant magnetoresistance effect in the magnetic superlattices, where the transport of spin-polarized electrons is affected by the spin state of the adjacent layer in heterostructures [31,32]. In our case, the electron transport with a certain spin state at $\mu$ seems to be affected by the spin configuration of the occupied levels below $\mu$, whereby the difference in exchange interaction strength in regions with different spin configurations is striking [33,34]. For example, if the electrons at $\mu$ have the same spin orientation as the spin majority of occupied LLs, i.e., regions (0), (II), and (IV) in $R_{xx}$ for $\nu = 5 + 1/2$, the total spin configuration of the 2DES is not perturbed due to an attractive exchange interaction between the alike spins. On the other hand, if the carriers at $\mu$ have the opposite spin orientation than the spin majority, i.e., regions (I) and (III), they can cause the disturbance to the ferromagnetic background. Such an exchange interaction is expected to increase the system's total energy. To minimize the effect of the disturbance, the entire 2DES is likely to form spin textures, which in some cases could be unconventionally ordered, such as those seen in Skyrmions or magnetic polarons. Therefore, the electrons with ↓ spins at $\mu$ are partially localized; i.e., they behave as if they were trapped at bound states having an effective large mass. In transport, the localization's signature is a low $R_{xx}$, since $R_{xx} \propto \sigma_{xx}$ due to $\sigma_{xy} \gg \sigma_{xx}$.

Several key parameters of ZnO heterostructure may affect the electron-electron interactions and thereby lead the formation of spin orders. For instance, a strong electron-electron interaction causes an 8-times-larger LL mixing in ZnO $[(e^2/\epsilon l_B)/\hbar\omega_c] = (16.6/\sqrt{B_\perp})$ than in GaAs. Also, a large ratio of exchange interaction to Zeeman energy $[(e^2/\epsilon l_B)/(g^*\mu_B B_{total})] = 60\sqrt{(B_\perp/B^2_{total})}$ may favor spin order formations. The screening, characterized by the Thomas-Fermi wave vector $q_{TF} = (2m^*e^2/4\pi\epsilon\epsilon_0\hbar^2)$, may also play an important role. For ZnO, $q_{TF} = 1.4 \times 10^9$ m$^{-1}$ and is larger than that in GaAs. It should be mentioned that the magnetic length $l_B \cong 25.8$ nm$/\sqrt{B_\perp} > 2\pi/q^{ZnO}_{TF}$ is the larger length scale for $B_\perp < 25$ T. This is reverse for GaAs 2DES ($2\pi/q^{GaAs}_{TF} = 30$ nm) and may suggest a different electron interaction regime in ZnO. Since ZnO parameters are comparable with Si and AlAs, our results can be important for 2DES transport studies in these materials.

In conclusion, we have studied the SdHOs in MgZnO/ZnO heterostructures and have identified a distinct transport behavior for ↑ and ↓ electron spin states. In a tilted magnetic field, $R_{xx}$ at half-integer $\nu$ increases gradually with the tilt angle for ↑-spin electrons, in accordance with the diffusive transport model. By contrast, $R_{xx}$ for ↓-spin electrons develops almost flat regions (plateaus) with a magnitude on the order of $R_{xx}$ at $B_{total} = 0$. In sharp contrast to the predictions of the diffusive transport model, the resistivity at plateaus is fairly independent of the tilt angle. This striking observation does not fit existing transport models and calls for theoretical understanding. One possible scenario could be that the underlying mechanism is related to the formation of nontrivial many-body states such as spin textures. The distinct behavior for two spin states is important not only for understanding the stabilization of fractional quantum Hall states in ZnO [35] but can also be used for development of ZnO-based electromagnetic devices.

We acknowledge a fruitful discussion with M. Kawamura, M. Onoda, M. Shayegan, H. Aoki, and N. Nagaosa. This work was partly supported by Grants-in-Aid for Scientific Research (S) No. 24226002 and No. 24224009 from MEXT, Japan, "Funding Program for World-Leading Innovative R&D on Science and Technology (FIRST)" Program from the Japan Society for the Promotion of Science (JSPS) initiated by the Council for Science and Technology Policy.

*maryenko@riken.jp

[1] V. Umansky, M. Heiblum, Y. Levinson, J. Smet, J. Nübler, and M. Dolev, J. Cryst. Growth **311**, 1658 (2009).
[2] L. Pfeiffer and K. W. West, Physica (Amsterdam) **20E**, 57 (2003).
[3] J. Falson, D. Maryenko, Y. Kozuka, A. Tsukazaki, and M. Kawasaki, Appl. Phys. Express **4**, 091101 (2011).
[4] I. M. Lifshitz and A. M. Kosevich, Zh. Eksp. Teor. Fiz. **29**, 730 (1955).
[5] V. M. Pudalov, M. E. Gershenson, and H. Kojima, Phys. Rev. B **90**, 075147 (2014).
[6] G. W. Martin, D. L. Maslov, and M. Y. Reizer, Phys. Rev. B **68**, 241309 (2003).
[7] Y. Adamov, I. V. Gornyi, and A. D. Mirlin, Phys. Rev. B **73**, 045426 (2006).
[8] S. Syed, M. J. Manfra, Y. J. Wang, R. J. Molnar, and H. L. Stormer, Appl. Phys. Lett. **84**, 1507 (2004).
[9] B. A. Piot, D. K. Maude, M. Henini, Z. R. Wasilewski, K. J. Friedland, R. Hey, K. H. Ploog, A. I. Toropov, R. Airey, and G. Hill, Phys. Rev. B **72**, 245325 (2005).
[10] W. Knap *et al.*, J. Phys. Condens. Matter **16**, 3421 (2004).
[11] M. M. Fogler and B. I. Shklovskii, Phys. Rev. B **52**, 17366 (1995).
[12] I. L. Aleiner and L. I. Glazman, Phys. Rev. B **52**, 11296 (1995).
[13] O. E. Dial, R. C. Ashoori, L. N. Pfeiffer, and K. W. West, Nature (London) **448**, 176 (2007).
[14] A. Tsukazaki, A. Ohtomo, T. Kita, Y. Ohno, H. Ohno, and M. Kawasaki, Science **315**, 1388 (2007).
[15] A. Tsukazaki, S. Akasaka, K. Nakahara, Y. Ohno, H. Ohno, D. Maryenko, A. Ohtomo, and M. Kawasaki, Nat. Mater. **9**, 889 (2010).
[16] K. Vakili, Y. P. Shkolnikov, E. Tutuc, N. C. Bishop, E. P. De Poortere, and M. Shayegan, Phys. Rev. Lett. **94**, 176402 (2005).
[17] A. Tsukazaki *et al.*, Phys. Rev. B **78**, 233308 (2008).
[18] Y. Kozuka, A. Tsukazaki, D. Maryenko, J. Falson, C. Bell, M. Kim, Y. Hikita, H. Y. Hwang, and M. Kawasaki, Phys. Rev. B **85**, 075302 (2012).
[19] D. Maryenko, J. Falson, Y. Kozuka, A. Tsukazaki, and M. Kawasaki, Phys. Rev. B **90**, 245303 (2014).
[20] D. R. Leadley, R. J. Nicholas, J. J. Harris, and C. T. Foxon, Phys. Rev. B **58**, 13036 (1998).
[21] F. F. Fang and P. J. Stiles, Phys. Rev. **174**, 823 (1968).
[22] D. Q. Wang, J. C. H. Chen, O. Klochan, K. Das Gupta, D. Reuter, A. D. Wieck, D. A. Ritchie, and A. R. Hamilton, Phys. Rev. B **87**, 195313 (2013).
[23] P. Moetakef, D. G. Ouellette, J. R. Williams, S. James Allen, L. Balents, D. Goldhaber-Gordon, and S. Stemmer, Appl. Phys. Lett. **101**, 151604 (2012).
[24] N. N. Klimov, D. A. Knyazev, O. E. Omel'yanovskii, V. M. Pudalov, H. Kojima, and M. E. Gershenson, Phys. Rev. B **78**, 195308 (2008).
[25] P. Svoboda, P. Středa, G. Nachtwei, A. Jaeger, M. Cukr, and M. Láznička, Phys. Rev. B **45**, 8763 (1992).
[26] R. J. Haug, Semicond. Sci. Technol. **8**, 131 (1993).
[27] See Supplemental Material at http://link.aps.org/supplemental/10.1103/PhysRevLett.115.197601 for details on the analysis of SdHO in Fig. 2 as well as sample details.
[28] T. Ando and Y. Uemura, J. Phys. Soc. Jpn. **36**, 959 (1974).
[29] I. A. Dmitriev, A. D. Mirlin, and D. G. Polyakov, Phys. Rev. Lett. **91**, 226802 (2003).
[30] Alternatively, $R_{xx}$ independent of $N_\downarrow$ might imply $1/E_{F\downarrow}$ scaling of the ratio $\tau_\downarrow(E_{F\downarrow})/\tau_{\rm tr}(E_{F\downarrow})$ for small $E_{F\downarrow} \sim (N_\downarrow + 1/2)\omega_c$, which, strictly speaking, does not contradict the energy-independent $\tau_\uparrow(E_{F\uparrow})/\tau_{\rm tr}(E_{F\uparrow})$ at large $E_{F\uparrow} \gg E_{F\downarrow}$ apparent from Fig. 4(c).
[31] M. N. Baibich, J. M. Broto, A. Fert, F. NguyenVanDau, F. Petroff, P. Etienne, G. Creuzet, A. Friederich, and J. Chazelas, Phys. Rev. Lett. **61**, 2472 (1988).
[32] G. Binasch, P. Grünberg, F. Saurenbach, and W. Zinn, Phys. Rev. B **39**, 4828 (1989).
[33] N. W. Ashcroft and N. D. Mermin, *Solid State Physics* (Brooks-Cole, Belmont, MA, 2005).
[34] G. F. Giuliani and J. J. Quinn, Phys. Rev. B **31**, 6228 (1985).
[35] J. Falson, D. Maryenko, B. Friess, D. Zhang, Y. Kozuka, A. Tsukazaki, J. H. Smet, and M. Kawasaki, Nat. Phys. **11**, 347 (2015).